# The unifying theory of scaling in thermal convection: The updated prefactors

**Richard J. A. M. Stevens [1,2], Erwin P. van der Poel [2], Siegfried Grossmann[3], and Detlef Lohse[2]**

[1]Dept. of Mechanical Engineering, Johns Hopkins University, Baltimore, Maryland 21218, USA
[2]Physics of Fluids Group, Faculty of Science and Technology, J.M. Burgers Center for Fluid Dynamics, and MESA+ Institute, University of Twente, 7500 AE Enschede, The Netherlands
[3] Fachbereich Physik, Philipps-Universität Marburg, Am Renthof 6, D-35032 Marburg, Germany

(Received 31 January 2013)

The unifying theory of scaling in thermal convection (Grossmann & Lohse (2000)) suggests that there are no pure power laws for the Nusselt and Reynolds numbers as function of the Rayleigh and Prandtl numbers in the experimentally accessible parameter regime. In Grossmann & Lohse (2001) the four dimensionless parameters of the theory were fitted to 155 experimental data points by Ahlers & Xu (2001) in the regime $3 \times 10^7 \leq Ra \leq 3 \times 10^9$ and $4 \leq Pr \leq 34$. Meanwhile the theory is on one hand well confirmed through various new experiments and numerical simulations. On the other hand these new data points provide the basis for an updated fit in a much larger parameter space. Here we pick four well established (and sufficiently distant) data points Nu(Ra,Pr) to obtain the four dimensionless constants $c_i$ of Grossmann and Lohse's unifying theory and show that the resulting Nu(Ra,Pr) function is in agreement with almost all established experimental and numerical data up to the ultimate regime of thermal convection, whose onset also follows from the theory. In addition, Re(Ra,Pr) is provided.

## 1. Introduction

Thermal convection is omnipresent in science and technology and its paradigmatical representation is Rayleigh-Bénard (RB) convection: a fluid in a sample heated from below and cooled from above. This system has received considerable attention in the last decades (Ahlers *et al.* 2009*b*; Siggia 1994; Lohse & Xia 2010), with one focus on the scaling properties of the global heat transport of the system. A now widely accepted viewpoint is the Grossmann-Lohse (GL) theory (Grossmann & Lohse 2000, 2001, 2002, 2004). The basis for this theory of scaling in RB convection are exact global balances for the energy and thermal dissipation rates derived from the Boussinesq equations and the decomposition of the flow in boundary layer (BL) and bulk contributions. The scaling of the dissipation rates in the BLs is assumed to obey Prandtl-Blasius-Pohlhausen scaling (Schlichting 1979), which is justified as long as the shear-Reynolds numbers of the BLs are not too large, and the scaling relations in the bulk are estimated based on Kolmogorov-type arguments for homogeneous isotropic turbulence. While the theory gives the different *scaling relations* for the individual contributions to the energy dissipation rates in the bulk and in the BL, namely $\epsilon_{u,bulk}$ and $\epsilon_{u,BL}$, and to the thermal dissipation rates in the bulk (background) and in the BLs (plus the plumes, see Grossmann & Lohse (2004)), namely $\epsilon_{\theta,bulk}$ and $\epsilon_{\theta,BL}$, the *absolute sizes* of these four relative

contributions are not given by the theory. They are expressed in four dimensionless prefactors $c_i$, $i = 1, 2, 3, 4$ for $\epsilon_{u,BL}$, $\epsilon_{u,bulk}$, $\epsilon_{\theta,BL}$, and $\epsilon_{\theta,bulk}$, respectively, which have to be adopted to experimental or numerical data for $Nu(Ra, Pr)$.

When the theory was developed early this century, such data were scarce and often contradicting each other, due to sidewall and plate effects, insufficient knowledge of the material properties of the fluid, lack of numerical resolution and other problems. Grossmann & Lohse (2001) used 155 data points for $Nu(Ra, Pr)$ in the parameter range $3 \times 10^7 \leq Ra \leq 3 \times 10^9$ and $4 \leq Pr \leq 34$ obtained by Ahlers & Xu (2001), which was the most extensive data set at that time. This fixed $Nu(Ra, Pr)$ for *all* $Ra$ and $Pr$, considered as valid up to the meanwhile found (He *et al.* (2012*b*)) ultimate regime of thermal convection, where the Prandtl-Blasius type BL becomes unstable. $Re(Ra, Pr)$ was fixed (cf. Grossmann & Lohse (2002)) with one extra adoption of the prefactor $a$ in the Prandtl-Blasius scaling relation $\lambda_u = aL/\sqrt{Re}$ to the experimental data of Qiu & Tong (2001), where $\lambda_u$ is the mean thickness of the kinetic BL and $L$ the height of the sample.

Although the data to which we adopted the four prefactors $c_i$ were relatively *local* in parameter space, the theory was rather successful in describing the *global* behavior $Nu(Ra, Pr)$ and also $Re(Ra, Pr)$, as described in detail in Ahlers *et al.* (2009*b*). This included the prediction that for $Pr \approx 1$ the onset to the ultimate regime should take place when Ra is of the order of $10^{14}$. This prediction was based on an assumed onset of a sheared BL instability at a shear Reynolds number $Re_s \approx 420$, which is the value given in Landau & Lifshitz (1987). Indeed, very recently He *et al.* (2012*b*) have found the onset of the ultimate regime at this very Rayleigh number.

Thanks to joint efforts of the community the experimental and numerical data situation for $Nu(Ra, Pr)$ has considerably improved in the last decade. Measurements have been extended to a much larger domain in the Ra-Pr parameter space, see the updated phase diagrams in figure 1 and figure 7, and plate- and sidewall corrections are much better understood and taken into account (Brown *et al.* (2005); Ahlers (2000); Roche *et al.* (2001); Verzicco (2002); Niemela & Sreenivasan (2003); Ahlers *et al.* (2009*b*)). Furthermore, due to the increasing computational power and better codes the numerical data are now well converged, confirming and complementing the experimental data. Meanwhile Stevens *et al.* (2010*c*, 2011*a*) achieved $Ra = 2 \cdot 10^{12}$ at $Pr = 0.7$ in a $\Gamma = 1/2$ sample and obtained a good agreement with the experimental data of He *et al.* (2012*b*) and Niemela *et al.* (2000).

This situation calls for a *refit* of the four prefactors $c_i$ of the GL theory, in spite of the success of the theory with the prefactors of Grossmann & Lohse (2001): It is clear that the surface $Nu(Ra, Pr)$ above the Ra-Pr parameter space will be much more stable and "wobble" less if we put it on four distant and trustable "legs" $Nu_i(Ra_i, Pr_i)$, $i = 1, 2, 3, 4$, rather than putting it on four "legs" somewhere in the center but close to each other. We emphasize that we obviously only need four such "legs" for the four constants. The shortcoming of the old set of $c_i$ was particularly obvious for small $Pr$, say $Pr \leq 1$ (see figure 5), because at the days of Grossmann & Lohse (2001) no reliable information was available in that parameter regime and therefore no Nusselt data of that regime had been included into the fit.

The structure of the paper is as follows: In section 2 we will provide the refit of the GL theory for an aspect ratio $\Gamma = 1$, leading to $Nu(Ra, Pr)$ in the whole parameter space up to the ultimate state. In section 3 we discuss the robustness of the fit. In section 3 we will show that this fit also describes the available data for $\Gamma = 1/2$ and will in particular discuss the onset of the ultimate regime. Section 4 gives conclusions and an outlook of the new challenges.

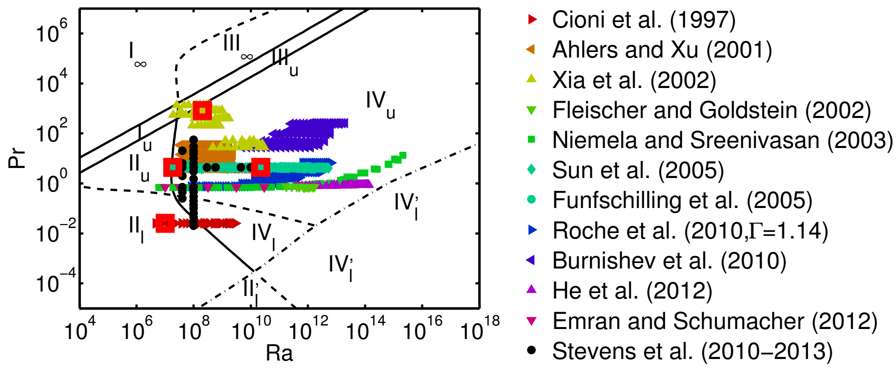


FIGURE 1. Phase diagram in $Ra - Pr$ plane for RB convection according to Grossmann and Lohse (Grossmann & Lohse (2000, 2001, 2002, 2004)) in a $\Gamma = 1$ sample with no-slip boundary conditions. The upper solid line means $Re = 1$; the lower nearly parallel solid line corresponds to $\epsilon_{u,BL} = \epsilon_{u,bulk}$; the curved solid and dashed line is $\epsilon_{\theta,BL} = \epsilon_{\theta,bulk}$; and along the long-dashed line $\lambda_u = \lambda_\theta$, i.e., $2aNu = \sqrt{Re}$. The dash-dotted line indicates where the laminar kinetic BL is expected to become turbulent, based on a critical shear Reynolds number $Re_s^* = 284$ of the kinetic BL, see text. The data are from Cioni *et al.* (1997); Glazier *et al.* (1999); Ahlers & Xu (2001); Fleischer & Goldstein (2002); Xia *et al.* (2002); Chaumat *et al.* (2002); Niemela & Sreenivasan (2003); Sun *et al.* (2005); Funfschilling *et al.* (2005); Roche *et al.* (2010); Burnishev *et al.* (2010); Emran & Schumacher (2012); He *et al.* (2012*a*); Stevens *et al.* (2010*b*,*a*); van der Poel *et al.* (2013). Note that for the Stevens et al. data points from different papers have been combined in the graph.

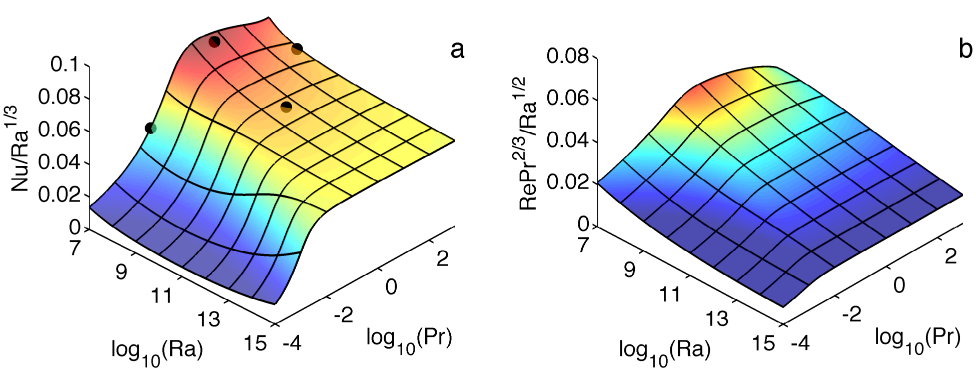


FIGURE 2. Compensated three-dimensional visualization of a) Nu(Ra,Pr) and b) Re(Ra,Pr). The four points used to fit the GL parameters $c_1 = 112.3161$, $c_2 = 67.6078$, $c_3 = 0.9318$ and $c_4 = 0.0921$ have been indicated by the black points in the Nu(Ra,Pr) graph.

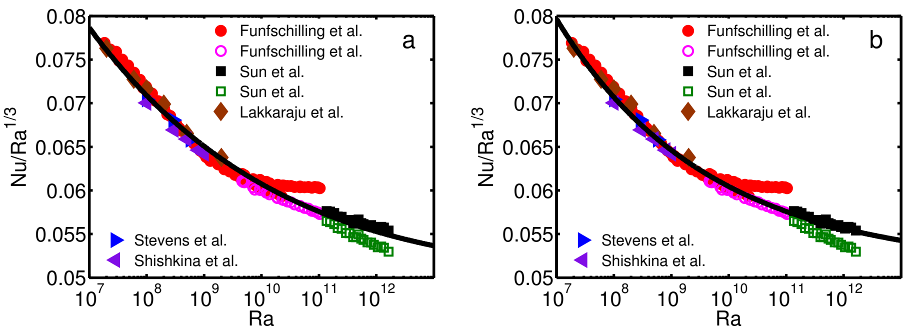


FIGURE 3. Comparison of the $Ra$-scaling of the original GL-fit from Grossmann & Lohse (2001) (a) with the new fit (b) for water, i.e. $Pr = 4.38$ unless mentioned otherwise, in a $\Gamma = 1$ sample. The circles (Funfschilling *et al.* (2005)) and squares (Sun & Xia (2005)) indicate experimental results. Open symbols indicate the uncorrected data and solid symbols the data after correction for the finite plate conductivity. The diamonds (Lakkaraju *et al.* (2012), $Pr = 5.4$), right pointing triangles (Stevens *et al.* (2011*b*)), and left pointing triangles (Shishkina & Thess (2009)) indicate results from numerical simulations.

## 2. Refit of the GL theory for $\Gamma = 1$

The GL theory describes Nu(Ra,Pr) and Re(Ra,Pr) with the following two coupled equations (Ahlers *et al.* (2009*b*)),

$$(Nu-1)RaPr^{-2} = c_1 \frac{Re^2}{g(\sqrt{Re_L/Re})} + c_2 Re^3, \tag{2.1}$$

$$Nu - 1 = c_3 Re^{1/2} Pr^{1/2} \left\{ f\left[ \frac{2aNu}{\sqrt{Re_L}} g\left(\sqrt{\frac{Re_L}{Re}}\right)\right]\right\}^{1/2} + c_4 Pr Re f\left[ \frac{2aNu}{\sqrt{Re_L}} g\left(\sqrt{\frac{Re_L}{Re}}\right)\right], \tag{2.2}$$

where the crossover functions f and g model the crossover from the thermal boundary layer nested in the kinetic one towards the inverse situation and from $\lambda_u = aL/\sqrt{Re}$ toward $\lambda_u \sim L$, respectively; for details, see Grossmann & Lohse (2001). As described by Grossmann & Lohse (2002) the prefactor $a = 0.482$ is obtained from the experimental data of Qiu & Tong (2001) and in addition we use $Re_L = 1.0$, where $Re_L$ is that Reynolds number for which the BL thickness according to Prandtl-Blasius is of order of the sample extension.

In order to get accurate values for the four dimensionless prefactors $c_i$ it is necessary to provide four data points with as much information about the richness of the RB system as possible, which means that data points from different regimes should be selected. Therefore we determined the $c_i$ from the data points of Funfschilling *et al.* (2005) at $Ra = 1.8\times10^7$ and $Ra = 2.25\times10^{10}$, both with $Pr = 4.38$, the data point from Xia *et al.* (2002) with $Pr = 818$ at $Ra = 2.04\times10^8$, and the data point from Cioni *et al.* (1997) at $Ra = 1\times10^7$ with $Pr = 0.025$. The location of these data points in the RB phase diagram is indicated by the large red squares in figure 1 and by the black dots in the corresponding three-dimensional Nu(Ra,Pr) visualization in figure 2a. Figure 1 shows that these data are indeed within different regimes. The reason for choosing these specific data points is two-fold. First of all we consider these four data point to be reliable. And apart from the data point by Xia *et al.* (2002), which is the only experiment in that large $Pr$ regime, all

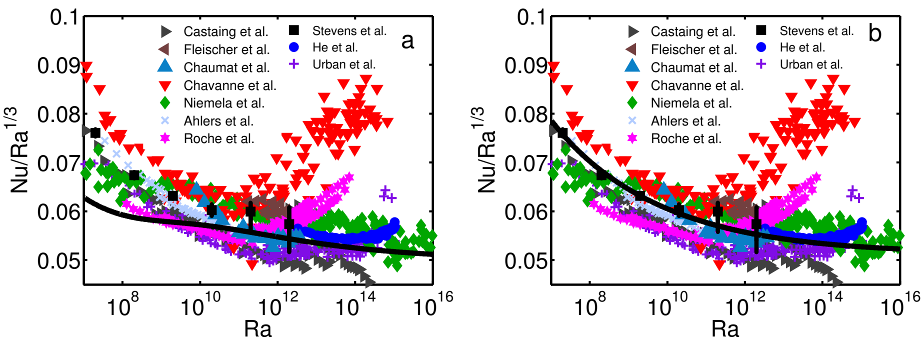


FIGURE 4. Comparison of the $Ra$-scaling of the original GL-fit from Grossmann & Lohse (2001) (a) with the new fit (b) in a $\Gamma = 1/2$ sample and varying $Pr$, see phase diagram in figure 7. The right pointing triangles are the experimental data from Castaing *et al.* (1989) with wall corrections Roche *et al.* (2010), left pointing triangles (Fleischer & Goldstein (2002)), upward pointing triangles (Chaumat *et al.* (2002)), downward pointing triangles (Chavanne *et al.* (2001)), diamonds (Niemela *et al.* (2000)), crosses (Ahlers *et al.* (2009*a*)), stars (Roche *et al.* (2010)), circles (He *et al.* (2012*b*); Ahlers *et al.* (2012*b*)), and plusses (Urban *et al.* (2011, 2012)) indicate experimental data and the squares results from numerical simulations (Stevens *et al.* (2010*c*, 2011*a*)).

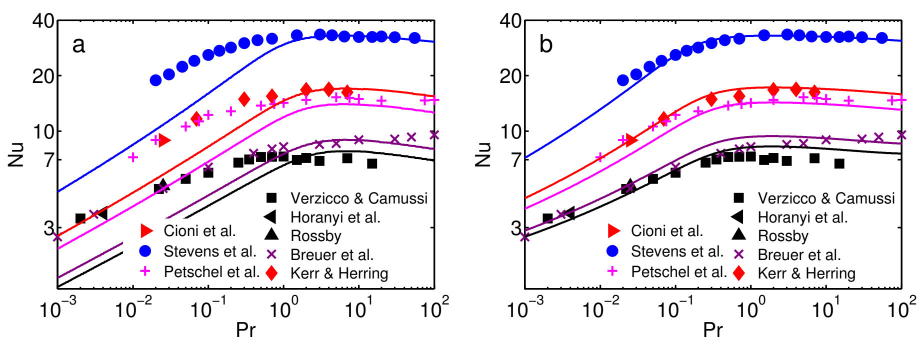


FIGURE 5. Comparison of the $Pr$-scaling of the original GL-fit from Grossmann & Lohse (2001) (a) with the new fit (b) for different $Ra$. The right pointing triangle (Cioni *et al.* (1997)), left pointing triangle (Horanyi *et al.* (1999)), and the upward pointing triangle (Rossby (1969)) indicate experimental results. The circles (van der Poel *et al.* (2013)) and squares (Verzicco & Camussi (1999)) indicate numerical results obtained in a cylinder with aspect ratio $\Gamma = 1$. The plusses (Petschel *et al.* (2013)) indicate numerical results obtained in a periodic domain and the diamonds (Kerr & Herring (2000)) and crosses (Breuer *et al.* (2004)) numerical results obtained in a box with free slip boundary condition at the sidewall. The colors black, purple, magenta, red, and blue (from bottom to top) corresponds to the $Ra$ numbers $5 \times 10^5$, $10^6$, $5 \times 10^6$, $10^7$, and $10^8$.

points agree very well with experimental or numerical data from other groups, see figures 3 and 5. In addition, these four data points are relatively far apart in the Ra-Pr parameter space to ensure that they provide the theory with as much information about the richness of the RB physics as possible. To provide information about the $Ra$-scaling we selected the measurements of Funfschilling *et al.* (2005) at $Ra = 1.8 \times 10^7$ and $Ra = 2.25 \times 10^{10}$ with $Pr = 4.38$. In order to include information about the transition between the 'upper' and 'lower' regimes, which is modeled by the crossover functions $f$ and $g$, it is necessary to provide data points in the low, intermediate, and high Pr number regime. We do this

selecting next to the intermediate Pr number data from Funfschilling *et al.* (2005), the low $Pr = 0.025$ number measurement by Cioni *et al.* (1997) at $Ra = 1 \times 10^7$ and the high $Pr = 1352$ measurement by Xia *et al.* (2002) at $Ra = 1.78 \times 10^9$. Altogether the four data points provide information from three different Pr numbers and four different Ra numbers. From these four data points we determine the $c_i$ with a fourth order Newton-Raphson root finding method and also by using a trust-region-reflective optimization. Both methods give $c_1 = 112.3161$, $c_2 = 67.6078$, $c_3 = 0.9318$ and $c_4 = 0.0921$.

In figures 3 to 5 we compare the GL-fit determined by Grossmann & Lohse (2001) with this new GL-fit, These figures clearly reveal that the new GL-fit is much closer to the data in the low $Pr$ number regime, while maintaining the similar excellent agreement for the high $Pr$ number data as before. We emphasize that this excellent agreement with the data from experiments and simulations that are not included in the fitting procedure, i.e. only four data points are used in the fitting procedure, confirms that the $c_i$ values we found describes $Nu(Ra, Pr)$ well in the regime that is nowadays covered by state of the art experiments and simulations. It is also noteworthy that figure 3 and 4 show that the Ra number scaling is perfectly predicted by the GL-theory for $Ra$ values that are decades higher than the highest $Ra$ number point that is used to determine the $c_i$ values, i.e. $Ra = 2.25 \times 10^{10}$, thus showing the predictive power of the GL-theory.

## 3. Robustness

To illustrate the robustness of the fit presented above, we show the results of a fit through four other data points, namely the data points from Funfschilling *et al.* (2005) at $Ra = 2.96 \times 10^7$ and $Ra = 1.92 \times 10^{10}$ with $Pr = 4.38$, the one from Xia *et al.* (2002) at $Ra = 2.24 \times 10^8$ with $Pr = 554$ and finally the data point by Kerr & Herring (2000) at $Ra = 10^7$ with $Pr = 0.07$. Three out of these four data points lie relatively close to the original four data points, but the low $Pr = 0.07$ point from Kerr & Herring (2000) substantially differs from the original $Pr = 0.025$. The reason that three of the four points are close to the original four points in the $Ra - Pr$ parameter space is that one can only select "reliable legs" in regimes were many measurements have been done and these regimes only cover a limited part of the parameter space.

The resulting GL coefficients are $c_1 = 114.1135$, $c_2 = 38.0299$, $c_3 = 0.9226$ and $c_4 = 0.0677$, compared to $c_1 = 112.3161$, $c_2 = 67.6078$, $c_3 = 0.9318$ and $c_4 = 0.0921$ of the fit described above. In order to compare the two fits we compare the relative difference in $Nu(Ra, Pr)$ calculated in the fit described in the previous section and $Nu$ calculated from this additional fit in the parts of the parameter space where the GL fit is valid. A comparison between both fits shows that the difference is very minor in the regimes $IV_u$, $II_u$, and $I_u$, and that the differences increase in the regimes $II_l$, $IV_l$, and $III_u$, which are very far away from the region in the parameter space where reliable data points are available. The reason is that a very small variation in the measurements point can lead to significant differences if the implied information is extrapolated over many decades in $Ra$ and $Pr$ using the GL-theory. For the fits compared here the differences increase up to about 10%.

## 4. GL theory for $\Gamma = 1/2$ and ultimate regime

In principle, the $c_i$ depend on the aspect ratio $\Gamma$. However, it is well known that only small differences in $Nu$ are observed between $\Gamma = 1/2$ and $\Gamma = 1$ (Ahlers *et al.* (2009*b*)). This weak aspect ratio dependence is confirmed by figure 4, which shows that the $Ra$ number scaling for $Pr = 0.7$ in a $\Gamma = 1/2$ sample is captured very accurately by the new

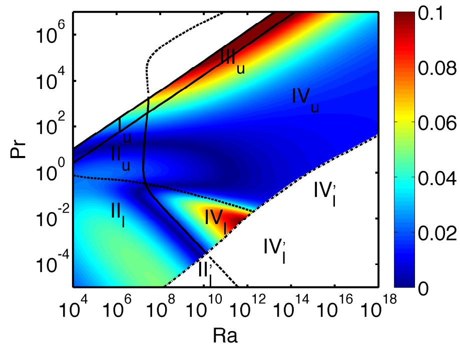


FIGURE 6. Relative difference between $Nu$ calculated from the original fit and $Nu$ calculated from the additional fit. The color scale ranges from blue to red, signifying 0% to 10% difference respectively.

fit for $\Gamma = 1$, and in the low Ra number regime the new fit is even much better than by the original fit of Grossmann & Lohse (2001).

The location in Ra-Pr space of the various regimes of the GL theory is based on the coefficients $c_i$. The updated lines that encompass the regimes are plotted in the phase diagrams shown in figures 1 and 7. The line that indicates the onset of the ultimate regime, where the kinetic boundary layer has become turbulent, is now based on the new $c_i$ and the transition at $Ra = 5 \cdot 10^{14}$, observed by He *et al.* (2012*b*) for $Pr = 0.86$. This gives $Re_s^* = 284$ instead of the previously used $Re_s^* = 420$ taken from pipe flow (Landau & Lifshitz (1987)). This new value for $Re_s^*$ is compatible with observations for flows along plates by Hansen (1928) and with the value 320 promoted by Niemela & Sreenivasan (2003).

The phase diagram in figure 7 shows that the measurements of He *et al.* (2012*b*) up to $Ra \approx 10^{15}$ at $Pr = 0.86$ are the only experiments that have reached the ultimate regime. They observe the onset of the ultimate regime at $Ra = 5 \cdot 10^{14}$ and a transition region for $10^{13} \leq Ra \leq 5 \cdot 10^{14}$. The experiments by He *et al.* (2012*b*) are the only room temperature experiments for $Ra \gtrsim 10^{12}$, while all other experiments that have reached these Ra numbers are low temperature experiments with Helium close to the critical point (Chavanne *et al.* (1997, 2001); Niemela *et al.* (2000, 2001); Niemela & Sreenivasan (2006); Roche *et al.* (2010); Urban *et al.* (2011, 2012)). In these low temperature experiments it is difficult to reach the ultimate regime because the Pr number increases with increasing Ra, see figure 7. Nevertheless the low temperature experiments by Niemela *et al.* (2000) seem to come very close to the ultimate regime and one may wonder why the transition region observed by He *et al.* (2012*b*) was not observed in the Niemela *et al.* (2000) experiments. We believe that the scatter of the Niemela *et al.* (2000) data at this highest Ra due to the uncertainties in the fluid properties in combination with the fact that the transition is smooth is the reason for this. Figure 4 shows that the scatter in the Niemela *et al.* (2000) data is similar to the trend observed in the transition regime. The phase diagram shows also shows that other low temperature experiments by Chavanne *et al.* (1997, 2001), Roche *et al.* (2010), and Urban *et al.* (2011, 2012) do not reach the ultimate regime and therefore no transition to the ultimate regime due to a BL shear instability is expected in these experiments.

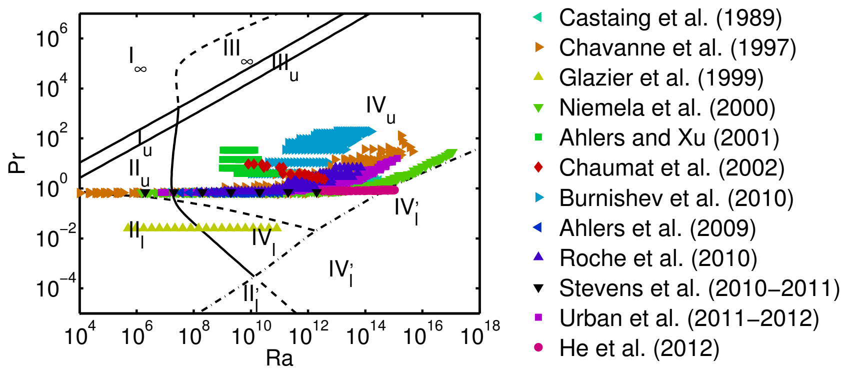


FIGURE 7. Phase diagram in $Ra - Pr$ plane for RB convection in a $\Gamma = 1/2$ sample with no-slip boundary conditions. The lines are the same as in figure 1. The data are from Castaing *et al.* (1989); Chavanne *et al.* (1997); Glazier *et al.* (1999); Niemela *et al.* (2000); Ahlers & Xu (2001); Chaumat *et al.* (2002); Ahlers *et al.* (2009*b*); Burnishev *et al.* (2010); Roche *et al.* (2010); Urban *et al.* (2011, 2012); He *et al.* (2012*b*); Stevens *et al.* (2010*c*, 2011*a*).

## 5. Conclusions and outlook

In this paper we have used the availability of new experimental and numerical data, and our increased understanding of the physics of the Rayleigh-Bénard system to determine the prefactors of the unifying theory for scaling in thermal convection, i.e. the Grossmann-Lohse theory, much more accurately. The resulting Nu(Ra,Pr) function is in very good agreement with almost all established experimental and numerical data up to the ultimate regime of thermal convection, and has significantly improved the predictions. In figure 4 one can notice the onset of the ultimate regime in the Nu(Ra) scaling of the measurements of He *et al.* (2012*b*). Extensions of the GL theory to the ultimate regime (see Grossmann & Lohse (2011)) are able to explain the observed Reynolds number scaling in the ultimate regime as well as the origin of the log-profiles Grossmann & Lohse (2012), observed in the ultimate regime Ahlers *et al.* (2012*a*).

In line with Grossmann & Lohse (2001), we have determined the prefactors from experimental measurements. This has great value as it shows that the information of only four data-points is sufficient to accurately predict Nu(Ra,Pr) up to the ultimate regime. All is based on the GL theory, which builds on exact global balances for the energy and thermal dissipation rates, derived from the Boussinesq equations, and the decomposition of the flow in boundary layer and bulk contributions.

A further challenge we want to pursue is to calculate the $c_i$ directly from the fluid equations, without the input of any experimental or numerical data, or at least quantitatively relate their values to important fluid concepts like Prandtl-Blasius-Pohlhausen theory, the von Karman-Prandtl theory, etc. in order to get an even deeper understanding of the GL theory.

## Acknowledgments

We thank all of our colleagues for various discussions over the years and G. Ahlers, F. Chilla, K. Petschel, P. Roche, L. Skrbek, R. Verzicco, K.-Q. Xia for providing us with their experimental and numerical data. Special thanks goes to G. Ahlers, K.-Q. Xia, and R. Verzicco. We acknowledge the foundation for Fundamental Research of Matter (FOM) for funding.

## REFERENCES

Ahlers, G. 2000 Effect of sidewall conductance on heat-transport measurements for turbulent Rayleigh-Bénard convection. *Phys. Rev. E* **63**, 015303–1 – 4.

Ahlers, G., Bodenschatz, E., Funfschilling, D., Grossmann, S., He, X., Lohse, D., Stevens, R.J.A.M. & Verzicco, R. 2012*a* Logarithmic temperature profiles in turbulent rayleigh-bénard convection. *Phys. Rev. Lett.* **109**, 114501.

Ahlers, G., Bodenschatz, E., Funfschilling, D. & Hogg, J. 2009*a* Turbulent Rayleigh-Bénard convection for a Prandtl number of 0.67. *J. Fluid. Mech.* **641**, 157–167.

Ahlers, G., Grossmann, S. & Lohse, D. 2009*b* Heat transfer and large scale dynamics in turbulent Rayleigh-Bénard convection. *Rev. Mod. Phys.* **81**, 503.

Ahlers, G., He, X., Funfschilling, D. & Bodenschatz, E. 2012*b* Heat transport by turbulent Rayleigh-Bénard convection for Pr=0.8 and $3 \times 10^{12} \leq Ra \leq 10^{15}$: aspect ratio $\Gamma$=0.50. *New J. Phys.* **14**, 063030.

Ahlers, G. & Xu, X. 2001 Prandtl-number dependence of heat transport in turbulent Rayleigh-Bénard convection. *Phys. Rev. Lett.* **86**, 3320–3323.

Breuer, M., Wessling, S., Schmalzl, J. & Hansen, U. 2004 Effect of inertia in Rayleigh-Bénard convection. *Phys. Rev. E* **69**, 026302.

Brown, E., Funfschilling, D., Nikolaenko, A. & Ahlers, G. 2005 Heat transport by turbulent Rayleigh-Bénard convection: Effect of finite top- and bottom conductivity. *Phys. Fluids* **17**, 075108.

Burnishev, Y., Segre, E. & Steinberg, V. 2010 Strong symmetrical non-OberbeckBoussinesq turbulent convection and the role of compressibility. *Phys. Fluids* **22**, 035108.

Castaing, B., Gunaratne, G., Heslot, F., Kadanoff, L., Libchaber, A., Thomae, S., Wu, X. Z., Zaleski, S. & Zanetti, G. 1989 Scaling of hard thermal turbulence in Rayleigh-Bénard convection. *J. Fluid Mech.* **204**, 1–30.

Chaumat, S., Castaing, B. & Chilla, F. 2002 Rayleigh-Bénard cells: influence of plate properties. In *Advances in Turbulence IX* (ed. I. P. Castro, P. E. Hancock & T. G. Thomas). Barcelona: International Center for Numerical Methods in Engineering, CIMNE.

Chavanne, X., Chilla, F., Castaing, B., Hebral, B., Chabaud, B. & Chaussy, J. 1997 Observation of the ultimate regime in Rayleigh-Bénard convection. *Phys. Rev. Lett.* **79**, 3648–3651.

Chavanne, X., Chilla, F., Chabaud, B., Castaing, B. & Hebral, B. 2001 Turbulent Rayleigh-Bénard convection in gaseous and liquid he. *Phys. Fluids* **13**, 1300–1320.

Cioni, S., Ciliberto, S. & Sommeria, J. 1997 Strongly turbulent Rayleigh-Bénard convection in mercury: comparison with results at moderate Prandtl number. *J. Fluid Mech.* **335**, 111–140.

Emran, M. S. & Schumacher, J. 2012 Conditional statistics of thermal dissipation rate in turbulent Rayleigh-Bénard convection. *Eur. Phys. J. E* **108**, 35.

Fleischer, A. S. & Goldstein, R. J. 2002 High-Rayleigh-number convection of pressurized gases in a horizontal enclosure. *J. Fluid Mech.* **469**, 1–12.

Funfschilling, D., Brown, E., Nikolaenko, A. & Ahlers, G. 2005 Heat transport by turbulent Rayleigh-Bénard convection in cylindrical cells with aspect ratio one and larger. *J. Fluid Mech.* **536**, 145–154.

Glazier, J. A., Segawa, T., Naert, A. & Sano, M. 1999 Evidence against ultrahard thermal turbulence at very high Rayleigh numbers. *Nature* **398**, 307–310.

Grossmann, S. & Lohse, D. 2000 Scaling in thermal convection: A unifying view. *J. Fluid. Mech.* **407**, 27–56.

Grossmann, S. & Lohse, D. 2001 Thermal convection for large Prandtl number. *Phys. Rev. Lett.* **86**, 3316–3319.

Grossmann, S. & Lohse, D. 2002 Prandtl and Rayleigh number dependence of the Reynolds number in turbulent thermal convection. *Phys. Rev. E* **66**, 016305.

Grossmann, S. & Lohse, D. 2004 Fluctuations in turbulent Rayleigh-Bénard convection: The role of plumes. *Phys. Fluids* **16**, 4462–4472.

Grossmann, S. & Lohse, D. 2011 Multiple scaling in the ultimate regime of thermal convection. *Phys. Fluids* **23**, 045108.

Grossmann, S. & Lohse, D. 2012 Logarithmic temperature profiles in the ultimate regime of thermal convection. *Phys. Fluids* **24**, 125103.

Hansen, M. 1928 Die geschwindigkeitsverteilung in der grenzschicht an einer eingetauchten platte. *Zeitschrift für Angewandte Mathematik und Mechanik* **8**, 185–199.

He, X., Funfschilling, D., Bodenschatz, E. & Ahlers, G. 2012*a* Heat transport by turbulent Rayleigh-Bénard convection for Pr=0.8 and $4 \times 10^{11} \leq Ra \leq 2 \times 10^{14}$ for aspect ratio Γ=1.00. *New J. Phys.* **14**, 103012.

He, X., Funfschilling, D., Nobach, H., Bodenschatz, E. & Ahlers, G. 2012*b* Transition to the ultimate state of turbulent Rayleigh-Bénard convection. *Phys. Rev. Lett.* **108**, 024502.

Horanyi, S., Krebs, L. & Müller, U. 1999 Turbulent Rayleigh-Bénard convection in low prandtl number fluids. *Int. J. Heat Mass Transfer* **42**, 3983–4003.

Kerr, R. & Herring, J. R. 2000 Prandtl number dependence of nusselt number in direct numerical simulations. *J. Fluid Mech.* **419**, 325–344.

Lakkaraju, R., Stevens, R.J.A.M., Verzicco, R., Grossmann, S., Prosperetti, A., Sun, C. & Lohse, D. 2012 Spatial distribution of heat flux and fluctuations in turbulent rayleigh-bénard convection. *Phys. Rev. E* **86**, 056315.

Landau, L. D. & Lifshitz, E. M. 1987 *Fluid Mechanics*. Oxford: Pergamon Press.

Lohse, D. & Xia, K. Q. 2010 Small-scale properties of turbulent Rayleigh-Bénard convection. *Annu. Rev. Fluid Mech.* **42**, 335–364.

Niemela, J., Skrbek, L., Sreenivasan, K. R. & Donnelly, R. 2000 Turbulent convection at very high Rayleigh numbers. *Nature* **404**, 837–840.

Niemela, J., Skrbek, L., Sreenivasan, K. R. & Donnelly, R. J. 2001 The wind in confined thermal turbulence. *J. Fluid Mech.* **449**, 169–178.

Niemela, J. & Sreenivasan, K. R. 2003 Confined turbulent convection. *J. Fluid Mech.* **481**, 355–384.

Niemela, J. & Sreenivasan, K. R. 2006 Turbulent convection at high Rayleigh numbers and aspect ratio 4. *J. Fluid Mech.* **557**, 411 – 422.

Petschel, K., Stellmach, S., Wilczek, M., Lülff, J. & Hansen, U. 2013 Dissipation layers in rayleigh-bnard convection: A unifying view. *arXiv:1212.5073* .

van der Poel, E. P., Stevens, R.J.A.M. & Lohse, D. 2013 Comparison between two and three dimensional Rayleigh-Bénard convection. *To be submitted to J. Fluid Mech.* .

Qiu, X. L. & Tong, P. 2001 Large scale velocity structures in turbulent thermal convection. *Phys. Rev. E* **64**, 036304.

Roche, P.E., Castaing, B., Chabaud, B., Hebral, B. & Sommeria, J. 2001 Side wall effects in Rayleigh-Bénard experiments. *Eur. Phys. J. B* **24**, 405–408.

Roche, P.-E., Gauthier, F., Kaiser, R. & Salort, J. 2010 On the triggering of the ultimate regime of convection. *New J. Phys.* **12**, 085014.

Rossby, H. T. 1969 A study of Bénard convection with and without rotation. *J. Fluid Mech.* **36**, 309–335.

Schlichting, H. 1979 *Boundary layer theory*, 7th edn. New York: McGraw Hill book company.

Shishkina, O. & Thess, A. 2009 Mean temperature profiles in turbulent Rayleigh–Bénard convection of water. *J. Fluid Mech.* **633**, 449–460.

Siggia, E. D. 1994 High Rayleigh number convection. *Annu. Rev. Fluid Mech.* **26**, 137–168.

Stevens, R. J. A. M., Clercx, H. J. H. & Lohse, D. 2010*a* Boundary layers in rotating weakly turbulent Rayleigh-Bénard convection. *Phys. Fluids* **22**, 085103.

Stevens, R. J. A. M., Clercx, H. J. H. & Lohse, D. 2010*b* Optimal Prandtl number for heat transfer in rotating Rayleigh-Bénard convection. *New J. Phys.* **12**, 075005.

Stevens, R. J. A. M., Lohse, D. & Verzicco, R. 2011*a* Prandtl number dependence of heat transport in high Rayleigh number thermal convection. *J. Fluid. Mech.* **688**, 31–43.

Stevens, R. J. A. M., Overkamp, J., Lohse, D. & Clercx, H. J. H. 2011*b* Effect of aspect-ratio on vortex distribution and heat transfer in rotating Rayleigh-Bénard. *Phys. Rev. E* **84**, 056313.

Stevens, R. J. A. M., Verzicco, R. & Lohse, D. 2010*c* Radial boundary layer structure and Nusselt number in Rayleigh-Bénard convection. *J. Fluid. Mech.* **643**, 495–507.

Sun, C., Ren, L.-Y., Song, H. & Xia, K.-Q. 2005 Heat transport by turbulent Rayleigh-

Bénard convection in 1m diameter cylindrical cells of widely varying aspect ratio. *J. Fluid Mech.* **542**, 165–174.

Sun, C. & Xia, K.-Q. 2005 Scaling of the Reynolds number in turbulent thermal convection. *Phys. Rev. E* **72**, 067302.

Urban, P., Hanzelka, P., Kralik, T., Musilova, V., Srnka, A. & Skrbek, L. 2012 Effect of boundary layers asymmetry on heat transfer efficiency in turbulent Rayleigh-Bénard convection at very high Rayleigh numbers. *Phys. Rev. Lett.* **109**, 154301.

Urban, P., Musilová, V. & Skrbek, L. 2011 Efficiency of heat transfer in turbulent Rayleigh-Bénard convection. *Phys. Rev. Lett.* **107**, 014302.

Verzicco, R. 2002 Sidewall finite conductivity effects in confined turbulent thermal convection. *J. Fluid Mech.* **473**, 201–210.

Verzicco, R. & Camussi, R. 1999 Prandtl number effects in convective turbulence. *J. Fluid Mech.* **383**, 55–73.

Xia, K.-Q., Lam, S. & Zhou, S. Q. 2002 Heat-flux measurement in high-Prandtl-number turbulent Rayleigh-Bénard convection. *Phys. Rev. Lett.* **88**, 064501.